arXiv:0903.2276v1 [cond-mat.str-el] 12 Mar 2009

Unstable Shastry-Sutherland phase in Ce_2Pd_2Sn

J.G. Sereni[1,*], M. Gomez-Berisso[1,*], A. Braghta[2,3], G. Schmerber[3] and J.P. Kappler[3]
[1] *Div. Bajas Temperaturas, Centro Atómico Bariloche (CNEA), 8400 S.C. Bariloche, Argentina*
[2] *Département de Physique, Université de Guelma, 24000 Guelma, Algeria*
[3] *IPCMS, UMR 7504 CNRS-ULP, 23 rue de Loess, B.P. 43 Strasbourg Cedex 2, France*

(Dated: March 13, 2009)

Thermal (C_P), magnetic (M and χ_{ac}) and transport (ρ) measurements on Ce_2Pd_2Sn are reported. High temperature properties are well described by the presence of two excited crystal field levels at (65 ± 5)K and (230 ± 20)K, with negligible hybridization (Kondo) effects. According to literature, two transitions were observed at $T_M = 4.8$K and $T_C = 2.1$K respectively. The upper transition cannot be considered as a standard anti-ferromagnetic because of frustration effects in a triangular network of Ce-atoms and the positive sign of the paramagnetic temperature $\theta_P^{LT} = 4.4$K. The nature of the this intermediated phase is described accounting for the formation of ferromagnetic (F) Ce-dimers disposed in a quasi-2D square lattice, resembling a Shastry-Sutherland pattern. According to hysteretic features in $\rho(T)$ and $\chi_{ac}(T)$, the lower F-transition is of first order, with $C_P(T < T_C)$ revealing a gap of anisotropy $E_g \approx 7$K.

PACS numbers: 71.20.LP; 74.25.Ha; 75.30.Mb

I. INTRODUCTION

The competition between different phases is resolved according to thermodynamic laws, being the configurational entropy an important factor to define the state of lower free energy (G) as the temperature is reduced. However, complex or meta-stable phases may occur since roughness in the G function of real systems may produce relative minima which become relevant. At the transition temperature, where the G minimum broadens according to the Ginsburg-Landau theory, the effect of exotic minima is favored. Within that context, there are non-trivial types of order, like frustration, incommensurability, glasses or even superconductivity related to quantum critical points, which may occur when the system does not accedes directly to an absolute minimum of energy.

The search of experimental examples where these conditions are realized is an important task in current investigations. The highest probability to find the mentioned conditions occurs in systems exhibiting multiple phase transitions because that situation reveals the competition between different configurations of comparable energy. According to literature, the Rare Earth based ternaries with the formula R_2T_2X are suitable candidates for such a purpose, as it was demonstrated by the study of the Yb_2Pd_2(In,Sn) system [1]. In this In/Sn doped compound, the stoichiometric limits are non-magnetic heavy Fermions whilst incipient magnetic order shows up at intermediate In/Sn substitution.

Crystal chemistry and magnetic properties of R_2T_2X compounds (with R=Ln [2, 3] and Ac [4], T=Transition Metals of the VIII group [2, 5, 6] and X=early p-metals [5]) have been investigated over the past two decades motivated by their peculiar crystalline structure and magnetic behaviors. Their tetragonal Mo_2FeB_2-type structure [4] is strongly anisotropic and can be described as successive 'T+X' (at z=0) and 'R' (at z=1/2) layers.

$Ce_{2\pm x}Pd_{2\pm y}X_{1\mp z}$ (with $x + y + z = 0$) show an extended range of solubility. This favors that different types of magnetic configurations with similar energy compete for the formation of different phases. In fact, by tuning small excess/deficit of the components (x, y, z) one can drive these compounds between Ferromagnetic (F) and Antiferromagnetic (AF) order. In $Ce_{2\pm x}Pd_{2\pm y}In_{1\pm z}$ alloys [3] for example, the existence of two magnetic branches (c.f. F- and AF-) was determined in the ternary phase diagram.

In the case of $Ce_2Pd_{2+x}Sn_{1-x}$ stannide [7] two transitions at $T_N = 4.7$K and $T_C = 3.0$K were reported. Neutron diffusion experiments [8] revealed a modulated character of this intermediate phase, with the local moments pointing in the 'c' direction and an incommensurate propagation vector $[qx]$ changes from 0.11 (at 4.2K) to 0.077 (at 2.8K). At that temperature it suddenly drops to $[qx = 0]$, becoming ferromagnetic.

Despite of these results there are some contradictory features in the low temperature behavior of this compound. For example, it is unlikely to expect a standard AF behavior in a triangular network of magnetic atoms under geometrical frustration constrains. Furthermore, the reported value of the paramagnetic temperature θ_P^{LT} is positive, and practically coincide with upper magnetic transition temperature [9]. These properties impose a revision of the proposed AF character of that phase. For that reason we will label the upper transition as T_M instead of T_N like proposed in the literature.

In this paper we present a thorough investigation on thermal, magnetic and transport properties between and room temperature on Ce_2Pd_2Sn. These results prove the local character of the Ce moments, allow to gain insight into the knowledge of the nature of intermediate phase at $T_M > T > T_C$ and the ferromagnetic character of the ground state.

II. EXPERIMENTAL DETAILS AND RESULTS

Since the magnetic properties of these compounds show a strong dependence on composition, we have chosen for this study a nearly stoichiometrc sample

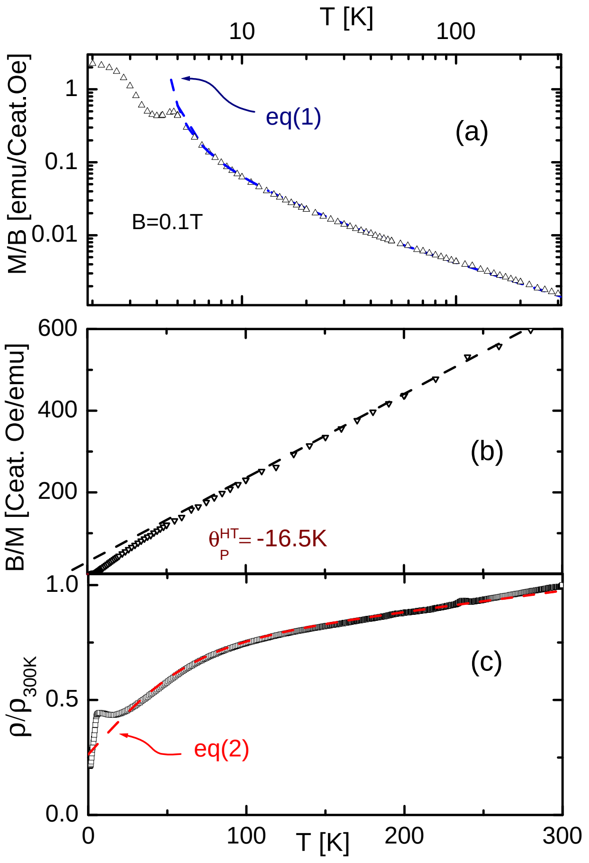

FIG. 1: High temperature properties of Ce_2Pd_2Sn. (a) thermal dependence of field normalized magnetization M/B in a double logarithmic representation. (b)Inverse magnetization B/M, with B=0.1T. Straight line represents the extrapolation from high temperature to extract θ_P^{HT}. (c) Temperature dependence of normalized electrical resistivity $\rho(T)/\rho_{300K}$. Dashed curves in (a) and (c) are fits using eq.(1) and (2) respectively, see the text.

with actual composition $Ce_{2.005}Pd_{1.988}Sn_{0.997}$ (after SEM/EDAX analysis). Details of sample preparation were described in a previous paper [9]. Lattice parameters study confirmed the single phase character of the sample with Mo_2FeB_2-type structure. The respective lattice parameters are: $a = 7.765\mathring{A}$ and $c = 3.902\mathring{A}$, with a $c/a = 0.5026$ ratio.

Electrical resistivity was measured between 0.5K and room temperature using a standard four probe technique with an LR700 bridge. DC-magnetization measurements were carried out using a SQUID magnetometer operating between 2 and 300K, and as a function of filed up to 5T. For AC-susceptibility a lock-in amplifier was used operating at 1.28KHz, with an excitation field of 1Oe on compensated secondary coils in the range of 0.5 to 10K. Specific heat was measured using the heat pulse technique in a semi-adiabatic He-3 calorimeter in the range between 0.5 and 20K, at zero and applied magnetic fields up to 4T.

A. High temperature results

High temperature DC-magnetization M/B and electrical resistivity ρ results are presented in Fig.1. The former is depicted as $M/B vs.T$ in a double logarithmic scale (Fig.1a), whilst the latter was normalized to the room temperature value ρ_{300K} (Fig.1c). Both curves are in good agreement with results obtained on similar samples [7, 10]. Fig.1b shows the inverse of the magnetization B/M used to extract the high temperature effective moment μ_{eff}^{HT} and paramagnetic Curie-Weiss temperature θ_P^{HT}.

$M(T)$ was measured up to room temperature with an applied field $B = 0.1$T. At $T_M = 4.8$K, it shows a cusp which was previously taken as an indication for an AF character of that transition. However, the divergent increase of $M/B(T \rightarrow T_I)$ with $T_I = 4.4$K, makes that argument uncertain. The analysis of these results can be done applying a simple formula [12]:

$$M/B = \sum_{0}^{2} \mu_i^2 * exp(-\Delta_i/T)/[(T - T_I) * Z] \qquad (1)$$

where μ_i are the effective moments of the ground state (i=0) and excited CF levels (i=1,2 respectively). Such a good fit in that wide range of temperature, with an equation only taking into account the Boltzmann thermal occupatio of the excited CF levels indicates that those levels very well defined in energy, excluding any significant "4f-band" hybridization effect.

The values obtained by applying this formula are: $\mu_0 = 1.7\mu_B$ and $\mu_1 = 1.9\mu_B$ and $\mu_2 = 2.48\mu_B$, and the respective CF splitting: $\Delta_1 = 65 \pm 4$K and $\Delta_2 = 230 \pm 20$K. Since at room temperature the upper CF level is not jet fully occupied, the value for a $J = 5/2$ moment is not reached.

The inverse of the susceptibility B/M shows a Curie-Weiss behavior at high temperature (i.e. $T \geq 80$K, see Fig.1b) with an extrapolation for the paramagnetic Curie-Weiss temperature: $\theta_P^{HT} = -16.5$K, in agreement with the literature [7]. However, below $T \approx 80$K a negative curvature takes over as the thermal population of the excited CF levels decreases. This results in a positive value of the low temperature extrapolation: $\theta_P^{LT} \rightarrow 4.4$K (see Fig.2a), in coincidence with the divergency at $T \rightarrow T_I$ in eq(1). The proximity of θ_P^{LT} to T_M is an evidence of a competition between different types of interactions, since the former is related to a F- divergence and the later to an AF-like cusp in $M(T)$.

$\rho(T)$ dependence can be described following the Matthiessen criterion: $\rho(T) = \rho_0 + \rho_m(T) + \rho_{ph}(T)$, where ρ_0 is the residual resisitivity, $\rho_m(T)$ the magnetic contribution and $\rho_{ph}(T)$ the phonon contribution to electronic scattering. Due to the mentioned negligible hybridization effects on the excited CF levels $\rho(T)$ is very well described by the simple expression [11], as shown in Fig.1c:

$$\rho(T) = a + b * tanh(T/D) + c * T \qquad (2)$$

where $a = \rho_0$, $b * tanh(T/D) = \rho_m$ and $c * T = \rho_{ph}(T)$. The parameter D indicates the characteristic energy

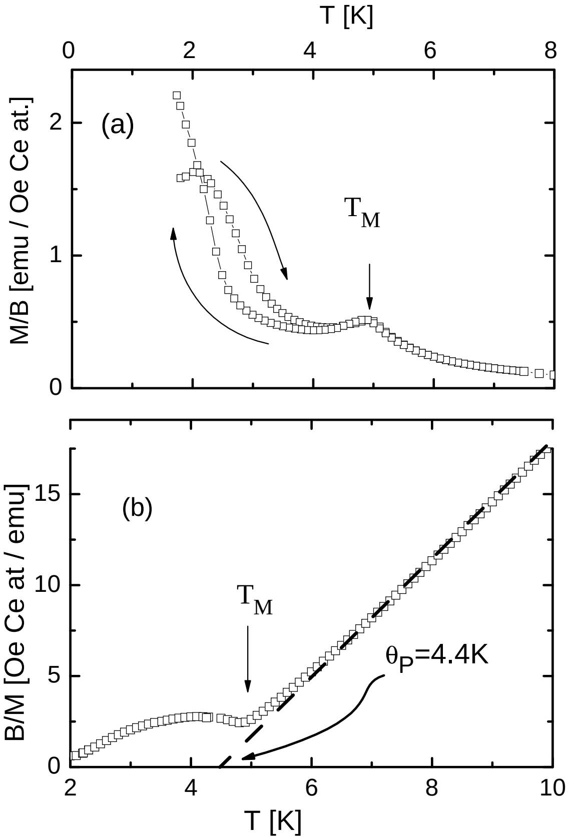

FIG. 2: (a) Comparison of Magnetization results in field (B=5mT) cooling (FC) and heating (after ZFC) processes. (b) Low temperature inverse magnetization B/M, with B=0.1T. Dashed line represents the extrapolation from high temperature to obtain θ_P^{LT}.

of the dominant scattering center, which in this case corresponds to the first excited crystal field (CF) level $\Delta_1 = 63$K. The second CF excited level can be estimated at $\Delta_2 > 200$K. These values are in good agreement with those extracted from $M/B(T)$.

B. Low temperature results ($T < 20\,$K)

As indicated by $M(T)$ results, the low temperature behavior of this compound is rather complex. Hence, some previous considerations are required to better understand the experimental results presented in this section. Since the AF molecular field (with $\theta_P^{HT} = -16.5$K) turns to ferromagnetic ($\theta_P^{LT} \rightarrow 4.4$K) below about 20K, one may distinguish a correlated-paramagnetic region between $20K > T > T_M$ from the canonical paramagnetism above that temperature. As mentioned before, despite of a cusp at $M(T_M)$ the upper transition is strongly affected by those F- type correlations. This situation persists in the intermediate phase ($T_M > T > T_C$)and it is only below T_C that the stable F- ground state is established.

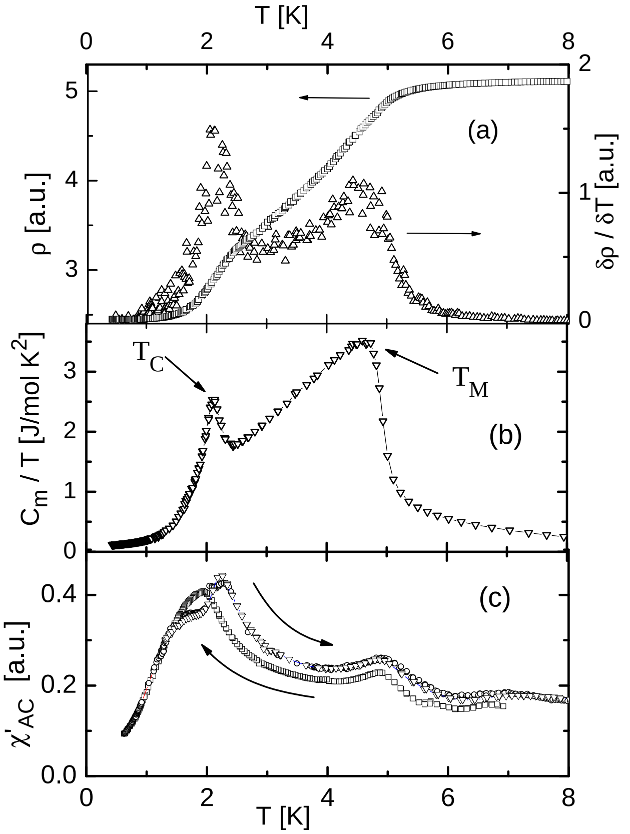

FIG. 3: (a) Low temperature electrical resistivity (left axis) and its temperature derivative (right axis). (b) Magnetic contribution to specific heat divided by temperature showing the upper (modulated) T_M and the lower (F) transitions. (c) AC-susceptibility as a function of temperature in cooling and (two runs) on heating procedures.

Between $20K > T > T_M$, $\rho(T)$ shows a slight increase which could be attributed to Kondo effect (see Fig.1c). Such an increase of $\rho(T \rightarrow T_M)$ might be attributed to Kondo effect, however, it is also observed above Ferromagnetic transitions, like in GdPt [13]. In that case, the increase of $\rho(T \rightarrow T_C)$ arises from F-fluctuations, precursors of the magnetic transition. Below T_M, $\rho(T)$ felts down without and sign of AF gap opening at the transition. At $T = T_C$, hysteretic effects are observed, which are practically suppressed by a field of nearly $0.2T$ (see Fig.2b).

Specific heat, $C_P(T)$, also shows an increasing contribution between $20 > T > T_M$ (see the Fig.3c) originated in magnetic correlations precursors of T_M transition. Since this $C_P(T > T_M)$ tail contains important information about the nature of the related transition, it will be analyzed in detail in the discussion section.

Modulated phase ($T_M > T > T_C$). $M(T)$ is certainly the most sensitive parameter to F-correlations. The low field (B=5mT) magnetization results shown in Fig.3a confirm the ambiguous behavior of the intermediate phase. The difference between cooling ($T \downarrow$)

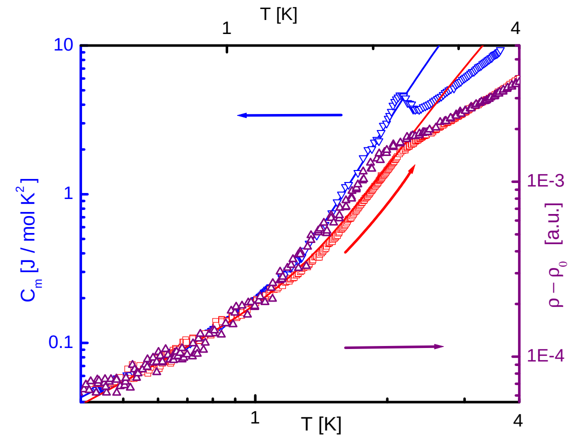

FIG. 4: Comparison of T dependencies of magnetic specific heat (left axis) and electrical resistivity (right axis) of the F-phase. Cooling and heating runs of resistivity show a hysteresis at T_C.

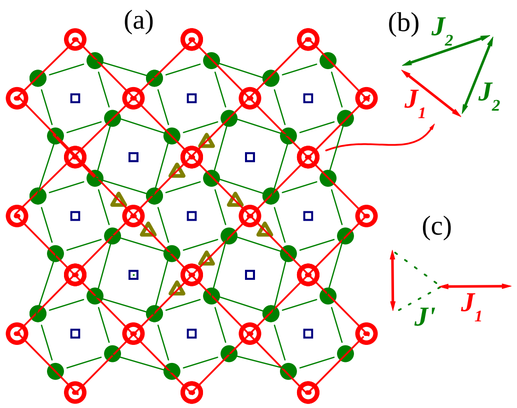

FIG. 5: (a) Mo_2FeB_2 type structure showing Ce (green ●), Sn (blue ☐) and Pd (yellow △) atoms. Superposed is a schematic representation of a square lattice (red lines) built up by F dimers (⊙) with moments pointing in the 'c' direction. (b) Magnetic interactions: J_1 (red) and J_2 (green), between Ce atoms on the 'ab' plane. (c) Magnetic interactions J' (green dots) between neighboring dimers.

and heating ($T \uparrow$) processes are evident, especially below $T_I = 4.4K (= \theta_P^{LT})$ which can be considered as a temperature of irreversibility. This means that the AF character proposed in the literature owing the modulated magnetic structure is never properly established.

Both magnetic transitions are determined from $C_m/T(T)$ measurements by the respective jumps at $T_M = 4.8$K and $T_C = 2.1$K respectively, as shown in Fig.3b. $C_m/T(T)$ is obtained after phonon subtraction extracted from La_2Pd_2Sn as: $C_m/T = C_P/T - C_P/T(La_2Pd_2Sn)$. The $C_m(T)$ dependence between $T_M \geq T \geq T_C$ does not fit into the expected for a canonical AF-, c.f. $C_m(T) \propto T^3$. Instead, the observed dependence: $C_m(T) = 0.5T^{2.25}$ is closer to that of a strongly anisotropic ferromagnet with $C_m(T) \propto T^{2.5}$ [14].

Ac-susceptibility χ_{ac} measurements, presented in Fig.3c, confirm these findings with an increasing signal below 4K and a maximum at T_C which depends on cooling or heating process and confirm hysteretic behavior.

Ferromagnetic phase ($T > T_C$). The hysteretic behavior between $T \downarrow$ (with χ_{ac}^{max} at $T \approx 1.9$K) and $T \uparrow$ (with χ_{ac}^{max} at $T \approx 2.2$K) indicates the first order character of the ferromagnetic transition. The lower limit of this hysteretic region is observed ≈ 1K. In the heating process, a shoulder is observed in $\chi_{ac}(T \uparrow)$ at $T \approx 1.5K$. This anomaly can be attributed to a very small amount of ferromagnetic Ce_3Pd_5 [15], which is not even detected in $C_P(T)$ nor in $\rho(T)$ measurements.

Also the temperature dependence of the electrical resistivity shows hysteretic behavior between cooling and heating around T_C as it can be seen in the inset of Fig.2. From specific heat results, the ferromagnetic transition occurs at $T_C = 2.1$K with sharp anomaly characteristic of first order type, which involve a small amount of latent heat.

Within the F- phase, both $C_m(T)$ and $\rho_m(T)$ are very well described by their respective F- temperature dependencies containing an exponential factor due to the presence of a gap in the magnon spectrum. Those functions are [16]:

$$C_m(T) = \gamma T + T^{3/2}(a + b\exp(-E_g/T)) \quad (3)$$

with $\gamma = 7mJ/molK^2$ confirming the absence of Kondo effect, and $E_g = 7.5$K. The electrical resistivity is well described by [17]:

$$\rho(T) \propto T^{1/2}\exp(-E_g/T)(1 + cT/E_g + d(T/E_g)^2) \quad (4)$$

with a similar value for the gap: $E_g = 7.2$K. The presence of this gap is a clear indication of the strong anisotropy of this system.

III. DISCUSSION

The strong local character of the "$4f$" orbital, as a well defined trivalent Ce atom, is concomitant with the irrelevant hybribization (or Kondo) effect on ground (GS) and CF excited states. Within such a scenario, a F- ground state is usually expected for Ce compounds [18]. Knowing that the twin compound $Ce_{2\pm x}Pd_{2\pm y}In_{1\pm z}$ modifies its magnetic structure with a slight variation of composition [3], one should ask whether the intermediate phase is an exotic phase appearing under this special situation of competing exchange interactions. Thus, the formation of such a phase previous to the stabilization of the F-GS rises the question about the role of the atomic configuration in this peculiar crystalline structure together with the consequent steric distribution of magnetic interactions. Accordingly, modulated/inconmensurated nature of the propagation vector hints for an exotic

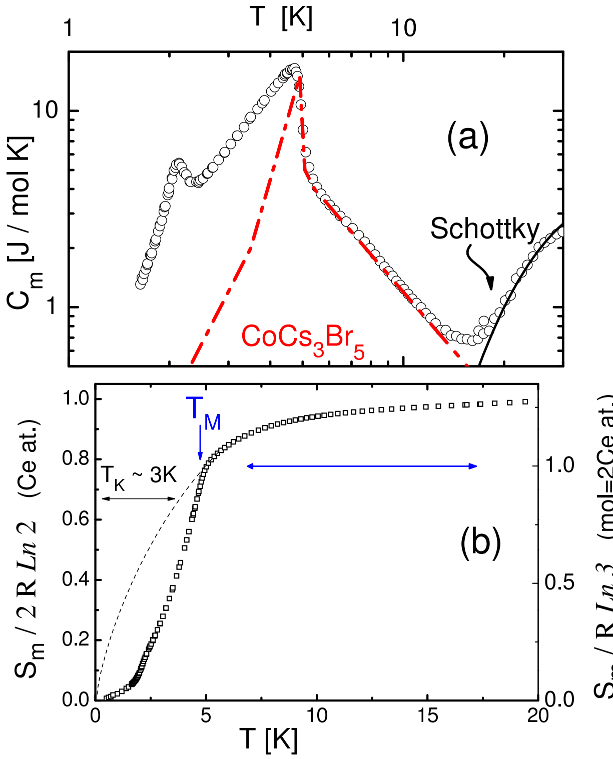

FIG. 6: a) Comparison of measured ”molar” specific heat tail at $T > T_M$ with that of an exemplary system of 2-D Ising S_{eff}=1 square lattice $CoCs_3Br_5$ [21]. b) Comparison of thermal entropy gain between $RLn2$ (right axis) and $RLn3$ (left axis) scales

character of that phase. Therefore, its origin should be searched mainly taking into account its structural properties rather than only the electronic ones.

Structural Properties The structural disposition of R atoms in these compounds can be depicted as trigonal and tetragonal prisms, centered around ‘T’ and ‘X’ atoms respectively, dispose the ‘R’ atoms in non centro-symmetric positions along the ‘c’ direction. As a consequence of the trigonal disposition, there a ”one to one” correlation of magnetic properties between Ce_2T_2X compounds and the correspondent CeT binary compounds [19] with CrB- or FeB-type structures (both structured in trigonal prisms [20]). This results in an assembled mosaic of rhombuses and squares projected on the basal plane. While the rhombuses are rotated $\pi/2$ respect to their four parent nearest-neighbors (nn), the squares are rotated $\pi/4$ among them (see Fig.5), mimetizing a sort of ”pinwheels” centered on the Sn-Sn column.

An important characteristic of this family of compounds is that the shortest d_{R-R} spacing (i.e. the nearest R-R neighbors, Rnn) can be either in the ‘c’ direction (2 nn) or in the basal ‘ab’ plane (1 nn) depending on the ‘c/a’ ratio of the lattice parameters. Values of $c/a < 0.5022$ favors the formation of a ‘R’ chains parallel to ‘c’, like in U_2Ni_2In [4]. On the contrary, for larger ’c/a’ values there is only one R-R first Rnn lying on the basal plane. Their distance is the shorter diagonal of the rhombus polygon (dashed line in Fig.7) and separates two triangular prisms disposed in mirror position, centered on the Pd-Pd column.

In Ce_2Pd_2Sn, the ratio c/a=0.5026 indicates that the nn is only one atom lying on the z=1/2 plane. However, the difference respect to the two next nn (in the ”c” direction) is less than 1%: $d_{Ce-1Ce} = 3.882 \AA$ and $d_{Ce-2Ce} = 3.902 \AA$ respectively. These two Ce-Ce spacings lie within the $3.7 < d_{Ce-Ce} < 4.0 \AA$ range where F-Ce binaries are placed [19], including CePd.

The nature of the modulated phase. To evaluate the consequences on these structural characteristics on the magnetic properties, one have to take into account that the effective RKKY interaction depends on three parameters:

$$J_{eff}(r) = J_{ex} * \mathbb{S}(\mathbb{S}+1) * f_{RKKY}(r) \qquad (5)$$

where J_{ex} is the intensity of the exchange interaction between $R - nn$ atoms, $\mathbb{S}$ represents the magnetic spin and $f_{RKKY}(r)$ is the RKKY oscillatory function. One have to consider different values of J_{ex} corresponding to each type of neighbor: J_1 and J_2 for the respective nn (one) and the next nnn (four) neighbors on the ‘ab’ plane, see Fig.5b. According to neutron measurements, J_c connecting Ce atoms with those of the upper and lower plane is not relevant in this range of temperature.

Although this compound shows its upper magnetic transition at $T_M = 4.8K$, the presence of magnetic correlations is observed at much higher temperatures in the tail of $C_m(T > T_M)$ and the increase of $\rho(T < 15K)$. These signs of incipient magnetic correlations within the paramagnetic phase contains important information about the nature of the transition itself since they contain the contribution of related precursors. Furthermore, strongly anisotropic or low dimensional systems display a significant amount of entropy above the transition. The existence of such a correlated paramagnetic region in the compound under study is confirmed by the fact that it has to be heated at least up to ≈ 20K for a ZFC process, otherwise traces of remand magnetic contributions are detected afterwards.

A deeper analysis of $C_m(T)$ shows that the temperature dependence at $T > T_M$ is $C_m \propto 1/T^2$, in coincidence with the specific heat of $CoCs_3Br_5$ [21] (see Fig.6a), which is an archetype for a quadratic spin $\mathbb{S}_{eff} = 1$ square lattice. Notice that not only the temperature dependence coincides but also their respective absolute values, provided that for Ce_2Pd_2Sn C_m is taken in ”mol” units (i.e. 2 Ce atoms). Notice that the transition temperature of the model compound is scaled to compound under study. The jump of the specific heat also points in that direction, since in mean field theory the jump of the specific heat at a magnetic transition is given by: $\Delta C_m = 2.5R[(2\mathbb{S}_{eff}+1)^2 - 1]/[(2\mathbb{S}_{eff}+1)^2 + 1]$ [22], which for $\mathbb{S}_{eff} = 1/2$ is $\Delta C_m = 1.5$R, whilst for $\mathbb{S}_{eff} = 1$ it becomes $\Delta C_m = 2$R like the measured value.

The magnetic entropy, computed as $\Delta S_m = \int C_m/T dT$, reaches the expected value $\Delta S_m = 2RLn2$ for a doublet ground state at around 15K (the pre-factor 2 corresponds to two magnetic atoms per formula unit). As depicted in Fig.5b, the entropy gain reaches 80% of that value at $T = T_M = 4.8$K. This is a direct consequence of the low value of $T_K \approx 3.0$K, which can be evaluated from $\Delta S_m(T)$ by applying the Desgranges-Schotte [23] criterion of $\Delta S_m(T = T_K) \cong 2/3RLn2$ for a non-ordered system.

The facts that, in the comparison with $CoCs_3Br_5$, the $C_m(T)$ of Ce_2Pd_2Sn has to be computed as "per mol" (i.e. = 2Ce at.) and that the reference compound has an effective spin $\mathbb{S}_{eff} = 1$, provide the keys to understand the physics of our compound. They suggest the formation of magnetic dimers built up through the J_1 interaction. Since the $\mathbb{S}_{eff} = 1$ momentum has three quantum projections, the measured entropy has to increase accordingly. In fact, the 80% of $\Delta S_m = 2RLn2$ (per Ce at.) collected up to $T = T_M$ corresponds to $0.5RLn3$ (i.e 'per mol'), as depicted on the right axis of Fig.5b. The 20% of the remanent value is related to the entropy relaxed in the $C_m(T > T_M)$ tail which arises from the difference between: $(Ln2 - 0.5Ln3)/Ln2)$.

The consequent structural loci of those dimers in a square lattice is sketched in Fig.4a, where the $\mathbb{S}_{eff} = 1$ moments are depicted in the center of the d_{Ce-1Ce} spacing as $\odot$. This structural configuration of dimers is topologically equivalent to the Shastry-Sutherland systems [24] proposed for AF dimers and inter-dimer interactions, i.e. AF J_1 and J'. As it was pointed out by theoretical calculations [25] Such combination of interaction can lead to a stable AF-GS, recently realized in Yb_2Pt_2Pb single crystals [26], which undergoes a slight shift of Pt atoms that results in two kinds of Yb-Pt tetrahedra.

Comparing these Yb and Ce isotypic compounds, we can remark the heavy fermion character of Yb_2Pt_2Pb, with $\gamma = 311\,\mathrm{mJ/mol\ K^2}$ [26], whereas the Ce one shows a record low value of $gamma = 7\,\mathrm{mJ/mol\ K^2}$. The hybridization effect may explain the lower entropy value of Yb_2Pt_2Pb at $T = T_N$ $[\Delta S_m(T_N) = 0.58RLn2]$ compared with that of Ce_2Pd_2Sn $[\Delta S_m(T_M) = 0.80RLn2]$. Among the similarities, one can mention the similar CF splitting of the first excited level ($\Delta_1 = 70\,$K and 65 K, respectively), though their $1/chi(T)$ curves show opposite signs. In both compounds, the extended tails above their respective upper transitions become significant at about three times T_N (T_M). At lower temperatures, they show an anomaly at nearly one half of the upper transition. Noteworthy is the fact that, while in Yb_2Pt_2Pb it looks like a shoulder (see Fig.5b in [26]), it is a first order transition in Ce_2Pd_2Sn.

Since in the compound under study J_1 is ferromagnetic, and that situation was not proved theoretically to become a stable GS, our magnetic scenario seems to be non trivial or perhaps even meta-stable. Furthermore, taking into account the modulated character of the intermediate phase, an AF interaction between dimers (i.e. J' in Fig.5c) can be expected. Particularly, in the case of Ce_2Pd_2Sn, the low temperature magnetic properties suggest that the proposed Ce-Ce magnetic dimerization arises once ΔS_m becomes $< RLn2$ (at $T \leq 20$K as suggested in Fig.6a) when the paramagnetic degrees of freedom of the doublet GS start to condense. Coincidentally, the straight line extrapolating $1/\chi$ to $\theta_P^{LT} = 4.4\,$K is well defined up to that temperature. However, when those dimers start to interact AF to each other via $J^{'}$ (as expected from the cusp of $M(T)$ at T_M), the long range order parameter cannot stabilize in a simple manner. Notice that only the couplings between *nn* dimers is depicted in Fig.5c for simplicity, whilst the Hamiltonian proposed in ref.[25] involves a set of next-*nn* couplings. This apparent intrinsic instability of the intermediate phase (probably originated in frustration effects) ends at the lower transition $T_C = 2$K, where a 3D F-GS takes over.

IV. CONCLUSIONS

These experimental results confirm Ce_2Pd_2Sn as one of the scars examples of ferromagnetic ground state among Ce intermetallic, with very stable magnetic moments and practically no traces of Kondo effect in the ground and excited CF states.

At intermediate temperatures ($T < 20$K) magnetic interactions develop with an excitation spectrum mimetizing a quasi-2D square lattice $\mathbb{S}_{eff} = 1$ model. This property, the entropy value at T_M $[\Delta S_m(T_M) = RLn3]$ and the structural morphology suggest the progressive formation of Ce-Ce ferromagnetic dimers within a pattern resembling that proposed by Shastry-Sutherland. The F character of J_1 is recognized from the positive value of θ_P^{LT} and the entropy related to a three fold degenerate state, whereas the AF character of the exchange $J^{'}$ between dimers explains the cusp of $M(T)$ at $T_M = 4.8\,$K. Nevertheless, this interaction is not able to stabilize the intermediate phase $(T_M \geq T \geq T_C)$ leading the system to another phase transition.

The comparison with isotypic Yb_2Pt_2Pb and model predictions suggest that no stable GS is reached in a combination of F-dimers (J_1) and AF exchange $(J^{'})$ among them, at least in this intermetallic compound. Nevertheless, an exotic phase with a non trivial order parameter compete in energy within a short range of temperature till the 3D F-GS takes over. At the Curie temperature $T_C = 2.1$K a first order transition is observed in $C_P(T)$, $\rho(T)$ and χ_{ac}, including hysteretic features. Below T_C, the $C_P(T)$ dependence reveals a gap of anisotropy $E_g \approx 7$K in the spectrum of mangnons.

Further measurements are in progress to investigate the magnetic phase diagram of Ce_2Pd_2Sn and the effect of a slight deviation from stoichiometry.

Acknowledgments

We are grateful to Dr.C.Geibel and M. Giovannini for clarifying discussions, and to Ms. Ogando for her participation in magnetic measurements. This work was partially supported by PIP-6016 (CONICET) and Secyt-UNC project 6/C256.
* J.G.S. and M.G-.B. are members of the Consejo Nacional de Investigaciones Científicas y Técnicas and Instituto Balseiro (UN Cuyo) of Argentina.

---

[1] E. Bauer et al., J. Phys.: Condens Matter 17 (2005) S999.

[2] F. Hulliger, J. Alloys & Comp. 221 (1995) L11.

[3] M. Giovannini et al., Phys. Rev. B 61 (2000) 4044.

[4] M.N. Peron et al., J. Alloys and Comp. 201 (1993) 203.

[5] R.A. Gordon et al., J. Alloys and Comp. 224 (1995) 101.

[6] D. Kacharovsky et al., Phys. Rev. B 54 (1996) 9891.

[7] F. Fourgeot et al., J. Alloys and Comp. 238 (1996) 102.

[8] D. Laffarge et al., Solid State Commun. 100 (1996) 575.

[9] A. Braghta et al., J. Magn. and Magn. Materials 320 (2008)1141.

[10] R.A. Gordon and F.J. Di Salvo, J. Alloys and Comp. 238 (1996) 57.

[11] J.G. Sereni et al., J. Phys.: Condens. Matter 18 (2006) 3789.

[12] J.G. Sereni et al., Phys. Rev. B 75 (2007) 024432.

[13] J.C. Gomez-Sal et al., Solid State Commun. 59 (1986) 771.

[14] A.I. Akhiezer et al., in *Spin waves*, North-Holland Series in Low Temperature Physics, Ed. C.J. Gorter, Vol I, ch. 6, p. 201, 1968, N-H Pub. Co.

[15] J.P. Kappler, M.J. Besnus, P. Lehmann, A Meyer and J.G. Sereni, J. Less-Comm. Metals 111 (1985) 261.

[16] L.J. Suntröm, in *Handbook for Physics and Chemistry of Rare Earths*, edited by K.A. Gschneidner Jr. and L. Eyring, Chap. 5, Vol 1 (Morth-Holland Pub. Co., 1978).

[17] See e.g. S.M Madeiros et al., Physica B 281 (2000) 340 and M.A. Continentino et al., Phys. Rev. B 64 (2001) 012404.

[18] J.G. Sereni, Physica B 215 (1995) 273.

[19] see for example: J.G. Sereni, in *Handbook for Physics and Chemistry of Rare Earths*, edited by K.A. Gschneidner Jr. and L. Eyring, Chap. 98, Vol 15 (Elsevier Science B.V, 1991).

[20] R. Kiessling, Acta Chem. Scandinavica 4 (1950) 209.

[21] R.F. Wielinga, H.W. Blöte, J.A. Roest, W.J. Huiskamp, Physica 34 (1967) 223.

[22] See e.g. J.G. Sereni, in *Encyclopaedia of Materials, Science Technology*, Ed. K.H. Buschow, Sub.Ed. E. Gratz, Vol. 5, I-Mag, Elsevier Sci.Ltd. (2001), p. 4986.

[23] H.-U. Desgranges and K.D. Schotte, Physics Letters 91A (1982) 240.

[24] B.S. Shastry and B. Sutherland; Physica 108B (1981) 1069.

[25] S. Miyahara and K. Ueda; Phys. Rev. Lett. 82. (1999) 3701.

[26] M. S. Kim, M.C. Bennett and M.C. Aronson; Phys. Rev. B 77 (2008) 144425.